Learning-Based Multifunctional Elbow Exoskeleton Control

Xiaofeng Xiong, Cao Danh Do, and Poramate Manoonpong, *Member, IEEE*

***Abstract*—In this article, we propose a learning-based model for multifunctional elbow exoskeleton control, i.e., assist- and resist-as-needed (AAN and RAN). The model consists of online iterative learning and impedance adaptation mechanisms for predictive and variable compliant joint control. The model was implemented on a lightweight (0.425 kg) and portable elbow exoskeleton (i.e., POW-EXO) worn by three subjects, respectively. The implementation relies only on internal pose (e.g., joint position) feedback, rather than physical compliant mechanisms (e.g., springs) and external sensors (e.g., electromyography or force), typically required by conventional exoskeletons and controllers. The proposed model provides a novel technique to achieve multifunctional exoskeleton control with minimal mechatronics and sensing. Interestingly, its RAN control and POW-EXO as a quantification means may reveal interactive (mechanical) impedance variance and invariance in human motor control.**

***Index Terms*—Force control, robotics and mechatronics, variable compliant control, wearable robots.**

I. Introduction

ELBOW assistance and exercise are important for restoring patients' motor functions and preventing athletes' injuries [1], [2]. Mechatronic systems (e.g., exoskeletons) have proven to be an effective means for improving performance and reducing economic costs [3], [4]. Exoskeletons can provide human limbs not only with assistant joint torques in rehabilitation, but also resistant torques for exercise. Although there are exoskeleton products and prototypes on markets and in labs [5], there is no learning-based model for portable multifunctional elbow exoskeleton control that online adapts to different wearers and tasks.

Most existing models focus on a single function, i.e., assistance or resistance [6], [7]. For instance, many models (e.g., reinforcement learning) have been developed to learn assistant strategies for upper limb exoskeleton control [8], [9]. However, none of these address the issue of portable multifunctional exoskeleton control with online impedance adaptation, i.e., assist- and resist-as-needed (i.e., AAN and RAN) functions. The functions have been implemented to provide compliant interactions between exoskeletons and wearers based on impedance and admittance control [10]. Impedance control produces exoskeleton joint torques based on pose (e.g., position) feedback, while admittance control generates joint positions in terms of force feedback [11].

Adaptive impedance/admittance is more suitable for exoskeleton control [12], compared to a fixed one for a single application. This is because such an adaptation can aid various wearers in different tasks (i.e., assistance and resistance). Additionally, in contrast to traditional controllers [10], [13], the adaptation enables exoskeletons to reach a compromise between tasks (e.g., trajectory tracking) and compliance. However, most existing learning impedance models rely heavily on additional external sensing such as electromyography (EMG) and force [14], [15]. Force instance, Meattini *et al.* [16] developed an EMG-driven method to close a human–robot control loop, thereby preventing complex pretraining procedures and imprecise force prediction for various wearers [17]. However, their method is subject to intrinsic sensing limitations such as prediction inaccuracy and abnormal EMG–torque relationship (see details in Section IV). Although some limitations can be addressed by introducing novel sensors, e.g., for measuring muscle circumference [12], their design and calibration are sophisticated. Such sophistication reduces usability and practicality in different applications. A detailed review of related compliant control and designs is presented in [5], [10], and [18]. Taken together, there is no advanced learning model for predictive compliant multifunctional elbow exoskeleton control without external sensing (e.g., EMG) and passive mechanisms (e.g., springs).

To address the problem, we propose a learning-based model to free compliant multifunctional exoskeleton control from external sensing (e.g., EMG) and passive compliant mechanisms (e.g., springs). The model consists of iterative learning and online impedance mechanisms for predictive and variable compliant exoskeleton control. The implementation relies only on

Manuscript received January 7, 2021; revised May 22, 2021 and August 4, 2021; accepted September 13, 2021. Date of publication October 5, 2021; date of current version April 1, 2022. This work was supported in part by the Human Frontier Science Program under Grant RGP0002/2017 (P.M. = Project Co-PI), in part by Brødrene Hartmanns under Grant A36775 (X.X. = Project PI), in part by Thomas B. Thriges under Grant 7648-2106 (X.X. = Project PI), and in part by the Vidyasirimedhi Institute of Science, and Technology (VISTEC, P.M. = Project PI) under a startup grant on bio-inspired robotics. *(Corresponding author: Xiaofeng Xiong.)*

Xiaofeng Xiong and Cao Danh Do are with the SDU Biorobotics, The Mærsk Mc-Kinney Møller Institute, University of Southern Denmark (SDU), 5230 Odense, Denmark (e-mail: xizi@mmmi.sdu.dk; cdd@mmmi.sdu.dk).

Poramate Manoonpong is with the Bio-Inspired Robotics, and Neural Engineering Lab, The School of Information Science, and Technology, Vidyasirimedhi Institute of Science, and Technology, Rayong 21210, Thailand (e-mail: poma@mmmi.sdu.dk).

Color versions of one or more figures in this article are available at https://doi.org/10.1109/TIE.2021.3116572.

Digital Object Identifier 10.1109/TIE.2021.3116572

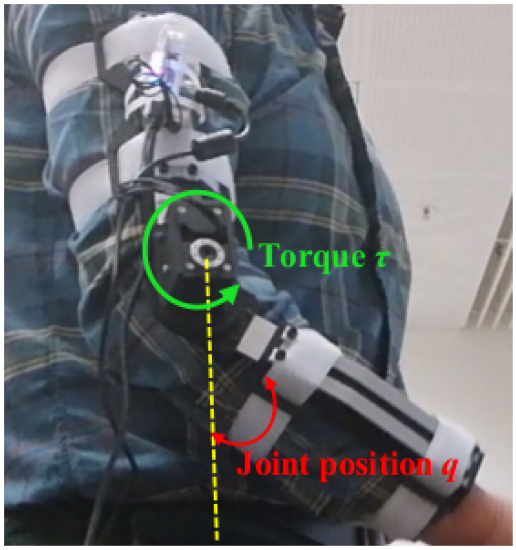

Fig. 1. Inverse dynamic model of an elbow exoskeleton (i.e., POW-EXO) and its wearer. The control torque of the POW-EXO is τ when its joint position is q [see (1) and (2)].

TABLE I
POW-EXO SPECIFICATION

Weight	Actuator	Stall torque	Voltage
0.425 $[kg]$	XM430	4.1 $[N \cdot m]$	12.0 $[V]$

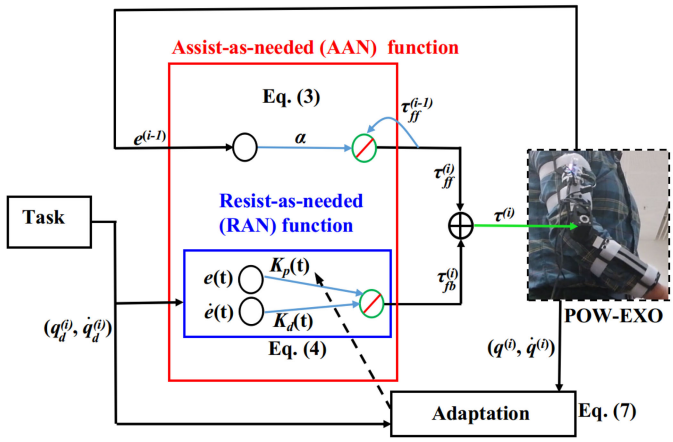

Fig. 2. Learning-based model for multifunctional elbow exoskeleton control. It consists of iterative learning [see (3)] and online impedance adaptation for predictive and variable compliant exoskeleton control. The dashed arrow line means that the impedance gains K_p and K_d are online adapted to involuntary and voluntary elbow movement [see (4) and (7)].

internal position and velocity feedback. The proposed model was validated on three healthy subjects wearing an elbow exoskeleton. "Multifunctional" here means that an exoskeleton can provide not only AAN physical support, but also RAN exercises; while typical exoskeleton control has been developed for a specific function, e.g., assistance [17]. The proposed AAN here focuses on assistant adaptations to various wearers, thereby online compensating for wearers' involuntary (i.e., reflex) involvement. This is different from traditional control which aims at maximizing wearers' involvement [13]. In contrast to the AAN, the proposed RAN here aims to maximize wearer's involvement in exercises. Note that the presented control and lightweight hardware are developed for portable assistance and resistance, rather than a single function performed by heavy multijoint ground-based exoskeletons [18]. To the best of our knowledge, the proposed model is the first to achieve learning-based multifunctional control of a portable exoskeleton with minimal (i.e., internal) sensing. The proposed model contributes to state of the art (SOA) by providing intelligent motion control for exoskeleton assistant and resistant tasks with minimal sensory feedback. It is a novel supplement to SOA exoskeleton designs and control [15], [19].

The rest of this article is structured as follows. The proposed learning-based control model (LBCM) is presented in Section II. Section III contains the experimental results of assistant and resistant tasks. Section IV concludes this article.

II. Learning-Based Model

The model consists of iterative learning and online impedance mechanisms for predictive and adaptive exoskeleton control. The model was validated using a lightweight (0.425 kg) wearable elbow exoskeleton (i.e., POW-EXO). The POW-EXO consists of 3-D printed polylactic acid parts, aluminum connectors, and a Dynamixel actuator (see Fig. 1 and Table I). Details of the exoskeleton design can be seen in [20].

The inverse dynamics model of the POW-EXO and its wearer (see Fig. 1) is given by [17]

$$I\ddot{q} + h(\dot{q}) + g(q) = \tau + \tau_h = \tau_s \tag{1}$$

where I, h, and g represent the unknown inertial, viscous, and gravity terms determined by exoskeleton joint acceleration $\ddot{q}$, velocity $\dot{q}$, and position q. The control input τ is generated by the learning-based model (see Fig. 2), compensating for the unknown exoskeleton dynamics (e.g., g) and interaction torque τ_h. τ is given by

$$\tau = -(\tau_{\text{ff}} + \tau_{\text{fb}}) \tag{2}$$

where τ_{ff} is iteratively learned for the intrinsic exoskeleton dynamics, while τ_{fb} is online adapted to the unknown interaction torque τ_h. Minus (i.e., '$-$') indicates the assistant torque τ (i.e., anticlockwise, see the green arrow in Fig. 1).

A. Iterative Learning Mechanism (ILM)

Iterative learning is a well-studied research field in robot-assisted applications. The ILM follows the proverb "practice makes perfect," facilitating better task performance than pure feedback control. This is because the ILM learns from previous trials to improve task performance. Moreover, it does not require much knowledge of controlled dynamics to design its learning gain. This advantage endows the ILM with greater flexibility in exoskeleton control, compared to feedback control. This is because the dynamics of an exoskeleton and its wearer intrinsically vary in accordance with different tasks. Therefore,

unknown exoskeleton dynamics are compensated by iteratively modulating the feedforward term τ_{ff} of the control input τ

$$\tau_{\text{ff}}^{i}(t) = \tau_{\text{ff}}^{i-1}(t) + \alpha e^{i-1}(t) \tag{3}$$

where the feedforward term τ_{ff} at time t of the ith iteration is determined by itself and position error e at the previous iteration [see e in (5). The learning gain α is empirically set to 0.1 for achieving fast stable control.

The principle of learning the feedforward term τ_{ff} is comparable to that used in human motor learning and control. Many human motor experiments have shown that humans learn to adapt to unknown dynamics in a predictive manner [21], [22]. Moreover, they adapt the mechanical impedance of their arms to position-based disturbances through sensory feedback (e.g., reflex) [23], [24]. Therefore, emulating such human motor learning requires the integration of predictive and adaptive learning control for unknown dynamics and different disturbances. Feedforward learning control can compensate for unknown dynamics, while control robustness against unexpected perturbations is enhanced by feedback-based online impedance adaptation.

B. Online Impedance Adaptation Mechanism (OIAM)

The OIAM is designed to generate the feedback joint torque τ_{fb} at a trial. τ_{fb} is governed by a proportional-derivative rule [20]

$$\tau_{\text{fb}} = K_p(t)e(t) + K_d(t)\dot{e}(t) \tag{4}$$

where $K_p(t)$ and $K_d(t)$ denote the impedance gains, while $e(t)$ and $\dot{e}(t)$ represent the joint position and velocity errors given by

$$e(t) = q(t) - q_d(t), \dot{e}(t) = \dot{q}(t) - \dot{q}_d(t), \varepsilon(t) = e(t) + \beta\dot{e}(t) \tag{5}$$

where $\varepsilon(t)$ denotes the joint tracking error with factor $\beta = 0.05$. In the OIAM, the impedance efforts and motion errors of the POW-EXO and its wearer are minimized over time period T given by [20]

$$\begin{aligned} J_o(t) &= J_c(t) + J_p(t) \\ J_c(t) &= \frac{1}{2}\int_{t-T}^{t} (K_p(t))^2 + (K_d(t))^2 \\ J_p(t) &= \frac{1}{2}\int_{t-T}^{t} V(t), V(t) = I(\varepsilon(t))^2. \end{aligned} \tag{6}$$

This minimization leads to online impedance adaptation given by

$$\begin{aligned} K_p(t) &= f(t)e(t), K_d(t) = f(t)\dot{e}(t) \\ f(t) &= \frac{\varepsilon(t)}{\beta(t)}, \beta(t) = \frac{a}{1 + b\varepsilon(t)^2} \end{aligned} \tag{7}$$

where $\beta(t)$ is an adaptation scalar with the positive scalars $a = 0.2$ and $b = 5$. The values of a and b are chosen to adapt the response speed. All scalars, as well as the derivation of (6) and (7), refer to our developed human-like impedance controller [25]. The stability proof of the online impedance adaptation law [i.e., (7)] can be seen in [25]. Note that the law has been validated in finger and elbow exoskeletons for exercise [20], [26], respectively.

C. Multifunctional Exoskeleton Control

The implementation consists of AAN and RAN control. Note that the AAN control is achieved by combining the ILM and OIAM, while only the OIAM is used for the RAN control (see Fig. 2). This is because only online impedance adaptation is required for the RAN control. The proposed control allows an elbow exoskeleton to provide the AAN and RAN to (stroke) patients in multistages [10], respectively. The AAN provides variable assistance to the patients with partial motor ability in repetitive exercises, in which their muscle controllability can be improved enough to initiate voluntary elbow movement. Further improvement will be facilitated by RAN exercises in late rehabilitation stage.

1) AAN Control: In the AAN, the desired exoskeleton joint position q_d is given by

$$q_d(t) = -\frac{\pi}{2.0}|\sin\left(\frac{4\pi}{15.0}t\right)|[\text{rad}], t \in [0, 15.0][\text{s}] \tag{8}$$

where 15.0 is the task time. Such desired position prevents elbow's overextension (i.e., $q_d(t) > 0$), thereby guaranteeing wearer's safety.

In AAN control, parameter θ is learned to minimize the position error given by

$$\begin{aligned} \text{minimize} \quad & |q_d - q(\theta)|, \theta = [\tau_{\text{ff}}, K_p, K_d]^T \\ \text{subject to} \quad & I\ddot{q} + h(\dot{q}) + g(q) = \tau_s(\theta) \\ & \tau_s(\theta) = \tau(\theta) + \tau_h, \tau(\theta) = -(\tau_{\text{ff}} + \tau_{\text{fb}}) \end{aligned} \tag{9}$$

where τ_s denotes the sensed torque of the POW-EXO actuator. The iterative learning and OIAMs are integrated for learning predictive (i.e., τ_{ff}) and adaptive [i.e., (K_p, K_d)] terms. Note that the AAN here enables the POW-EXO to generate motion assistance for compensating for involuntary (i.e., reflex) movement by various wearers. This is different from the conventional AAN control that aims at maximizing wearers' involvement.

2) RAN Control: Unlike the proposed AAN, only the adaptive terms K_p and K_d of the OIAM are online tuned for various exercisers. Therefore, the resistant torque is given by [rewritten from (2)],

$$\tau = -\tau_{\text{fb}}. \tag{10}$$

This is because its desired exoskeleton joint position is fixed as

$$q_d(t) = 0.0. \tag{11}$$

In contrast to the ANN, there is no cyclic tracking task. Moreover, the OIAM acts only as a virtual adjustable spring and damper for exercises. Greater resistant torque (i.e., τ) results from larger joint position (i.e., $|e|$) and velocity (i.e., $|\dot{e}|$) errors [see (7)]. In the RAN control, parameter Ω is online modulated to maximize wearer's exercise involvement quantified by

$$\begin{aligned} \text{maximize} \quad & |\tau_s(\Omega)|, \Omega = [K_p, K_d]^T \\ \text{subject to} \quad & I\ddot{q} + h(\dot{q}) + g(q) = \tau_s(\Omega) \\ & \tau_s(\Omega) = \tau(\Omega) + \tau_h, \tau(\Omega) = -\tau_{\text{fb}}(\Omega). \end{aligned} \tag{12}$$

III. Experiments

The AAN and RAN control was validated on the POW-EXO worn by three healthy subjects[1] (i.e., S1–S3; see the experimental video link in [27]). The subjects were not physically supported by any ground-based framework, since the POW-EXO is a body-based exoskeleton [18].

A. AAN Control

In the experiments, three subjects were asked to relax their muscles so as not to produce elbow joint torques. AAN torques were produced by the proposed model and POW-EXO, flexing and extending elbows to track a desired trajectory [see (8)]. However, their involuntary (i.e., reflex) movements were not completely prevented, leading to the unknown interaction torque τ_h [see (1)] deviating from the trajectory. Moreover, such deviations were affected by uncertainties such as muscle fatigue and unrepeatable involuntary movement. Therefore, the proposed control aims at compensating for wearers' involuntary movement to minimize the position error [see (9)]. This minimization is based on modulating the predictive (i.e., $\tau_{\rm ff}$) and adaptive (i.e., K_p and K_d) terms of the proposed model. The model was run for 16 trials on each subject.

The learning-based control starts at the feedback control without feedforward control [i.e., $\tau_{\rm ff}^1 = 0.0$; see Fig. 3(b)] in the first trial. We can see that the feedforward torque $\tau_{\rm ff}$ increases, while the feedback $\tau_{\rm fb}$ decreases over the learning trials (e.g., see the magenta area in Fig. 3). The decreased feedback $\tau_{\rm fb}$ results from a reduction in task error e. The increased feedforward and decreased feedback contributions by the proposed model guarantee the online control predictivity and adaptivity of the POW-EXO. As a result, the co-contributions reduce the average position error $\bar{e}$ over trials (see the blue line in row 1 of Fig. 4). The average joint position error $\bar{e}$ is given by [9], [13]

$$\bar{e}^i = \frac{\sum_{t=1}^{t=m} |q^i(t) - q_d^i(t)|}{m} [\text{rad}] \tag{13}$$

where i is the trial ID, and m is the time step. A small $\bar{e}$ indicates good AAN control.

The proposed control enables the POW-EXO to online learn the predictive (i.e., $\tau_{\rm ff}$) and adaptive (i.e., K_p and K_d) terms in the AAN tasks (see rows 2–4 of Fig. 4). As a result, it leads to variable predictive and compliant motion adaptation for various wearers. We can see that the medians of $\tau_{\rm ff}$, K_p, and K_d increase from subjects S1 to S3. Moreover, the deviation of the predictive (i.e., $\tau_{\rm ff}$) term is larger than those of the adaptive (i.e., K_p and K_d). This is because the learning-based control starts with online impedance adaptations. By contrast, its predictive learning is initialized from scratch (i.e., $\tau_{\rm ff}^1 = 0.0$). In the proposed model, iterative learning and OIAMs compensate for unknown dynamics and interaction of human–exoskeleton shared control, respectively. Note that the proposed learning-based control focuses on AAN adaptations for various wearers, rather than traditional AAN control for maximizing wearer's involvement [13].

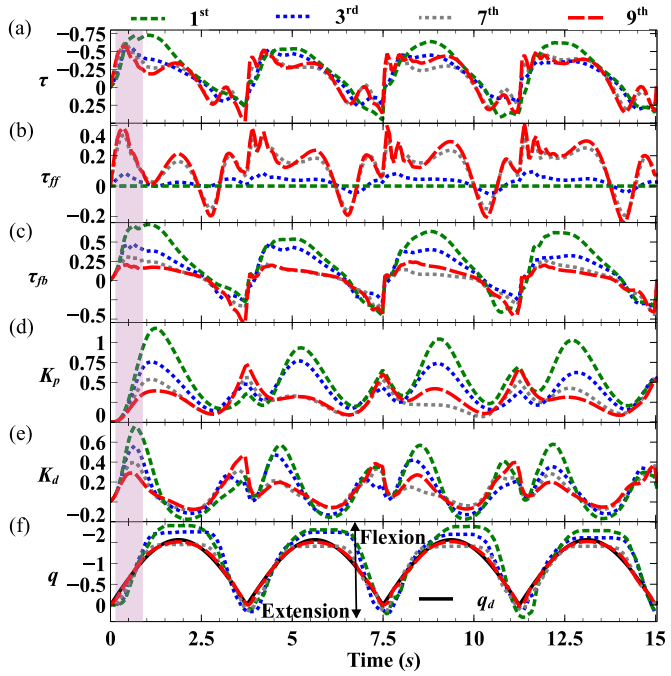

Fig. 3. Learning-based control for the POW-EXO in repetitive (i.e., elbow flexions and extensions) and AAN movements [see (8)]. The control was run on the POW-EXO worn by subject S1. The results before learning are shown in the first and third trials, while those after learning are presented at the seventh and ninth trials. (a)–(c) Control τ, feedforward $\tau_{\rm ff}$, and feedback $\tau_{\rm fb}$ torques. (d) and (e) Impedance parameters K_p and K_d. (f) Real q and desired q_d joint positions [see (8)]. The average joint position error $\bar{e}$ is indicated by the blue line in row 1 of Fig. 4.

B. RAN Control

Unlike the AAN control, the RAN aims at maximizing wearers' involvement [i.e., $|\tau_s|$, see (12)] only using the OIAM (see Section II-B). In the experiments, three subjects were asked to flex their elbows as much as possible. In elbow flexions, the resistant torque τ increases with rising flexion angles and velocities, resulting in large impedance terms K_p and K_d [see (7)]. Therefore, K_p and K_d of the OIAM are online adapted to generate variable resistance against different wearers. The OIAM acts as a virtual adjustable spring and damper [see (4)].

For instance, the OIAM enables the POW-EXO to produce variable resistant torque τ against subjects S2 and S3 via online modulating the impedance terms K_p and K_d [see Fig. 5(a)–(c)]. The resistance increases with the rising impedance terms (see the green area in Fig. 5). The online resistance adaptation control is smooth, because its impedance terms are online modulated based on a stable control law [see (7)]. According to the law, the impedance terms K_p and K_d increase with the increments of $|e|$ and $|\dot{e}|$, respectively. Interestingly, the prolonged repetitions

[1]The subjects consent to the participation in the experiments, which have been approved by the Research Ethics Committee of the University of Southern Denmark (case no.: 20/70421).

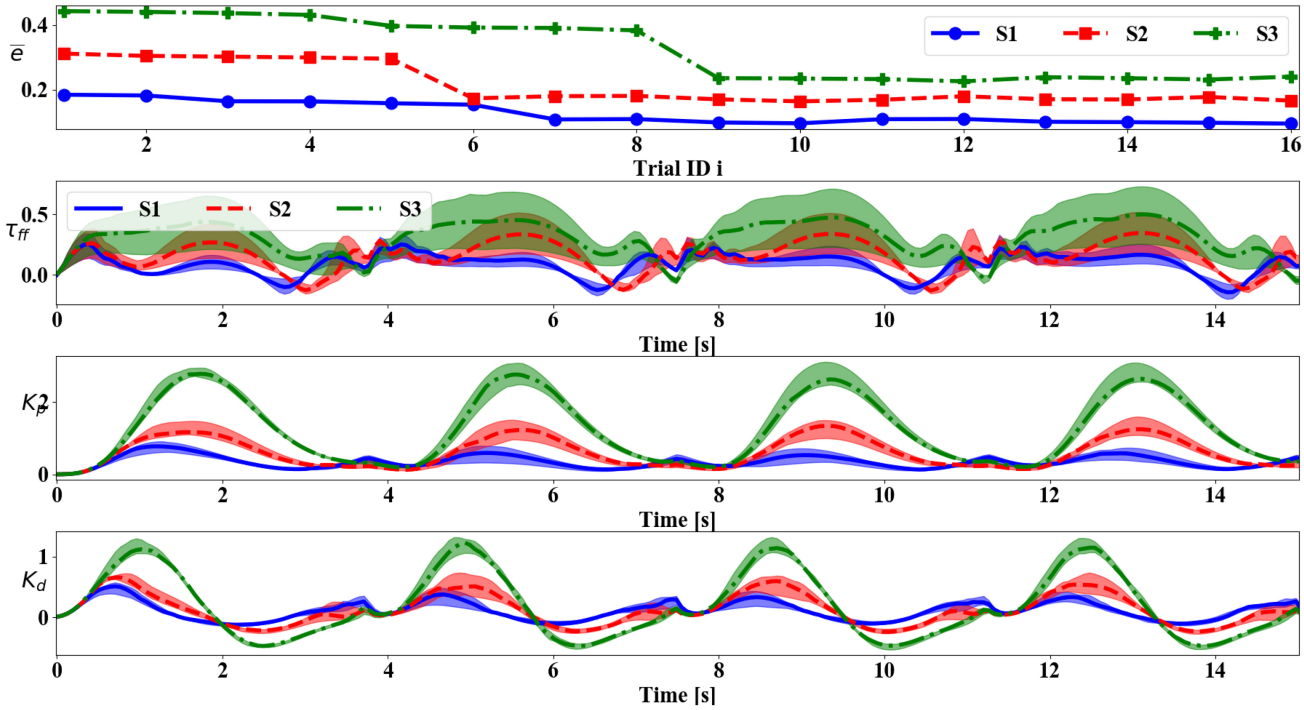

Fig. 4. Statistical results of the proposed model for AAN tasks. In the tasks, three subjects (i.e., S1–S3) wore the POW-EXO, and 16 trials were run for each subject. Rows 1–4 illustrate the average position error $\bar{e}$ [rad], the medians and deviations of learned feedforward torque τ_{ff}, and impedance parameters K_p and K_d. Blue, red, and green colors depict the results of subjects S1–S3, respectively.

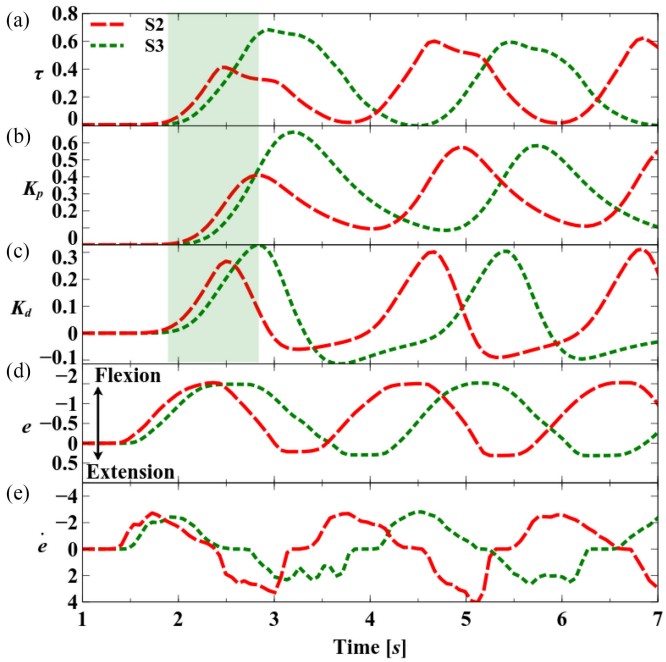

Fig. 5. Variable resistance against subjects S2 and S3 in exercises (i.e., elbow flexions and extensions). (a) Control τ. (b) and (c) Impedance parameters K_p and K_d. (d) and (e) Position e and velocity $\dot{e}$ errors. The green area illustrates the resistant torque τ increasing with the impedance terms K_p and K_d.

with large position and velocity deviations result in strong resistances (see S3 in Fig. 5). These resistances are led by the rising impedance gains K_p and K_d in terms of their online adaptation law [see (7)]. The wearers' involvement was maximized through the OIAM. The subject's exercise involvement is quantified by [10], [28]

$$\overline{\tau}_s^i = \frac{\sum_{t=1}^{t=m} |\tau_s(t)|}{m} \tag{14}$$

where i is the trial ID, and m is the time step. A deep involvement is indicated by a strong torque feedback (i.e., τ_s). We can see that subject S1 obtained deeper involvement, compared to other subjects (see row 1 of Fig. 6). Such involvement results from larger impedance terms (i.e., K_p and K_d, see rows 2 and 3 of Fig. 6). The resulting impedance terms and resistant torque τ increase with rising position and velocity errors (see rows 4 and 5 of Fig. 6), leading to strong torque feedback (i.e., τ_s). Therefore, the OAIM makes the POE-EXO generate RAN elbow motions against various wearers in exercises (see Fig. 7).

Interestingly, the proposed RAN control allows the exoskeleton to quantify the mechanical impedance of interactive elbow control. This quantification indicates that interactive impedance of elbows may vary over time [see $K_p(t)$ and $K_d(t)$ in Fig. 6], but eventually their averages converge at specific ranges [see $\overline{K_p}(t)$ and $\overline{K_d}(t)$ in Figs. 8 and 9]. The indication may reveal interactive mechanical impedance variance and invariance in human motor control [23], [24]. Here, the average mechanical impedance $\overline{K_p}(t)$ and $\overline{K_d}(t)$ are given by

$$\overline{K_{p,d}}(t) = \frac{\overline{K_{p,d}}(t-\Delta t)(n-1) + K_{p,d}(t)}{n}, \Delta t \approx 0.06(\text{s}) \tag{15}$$

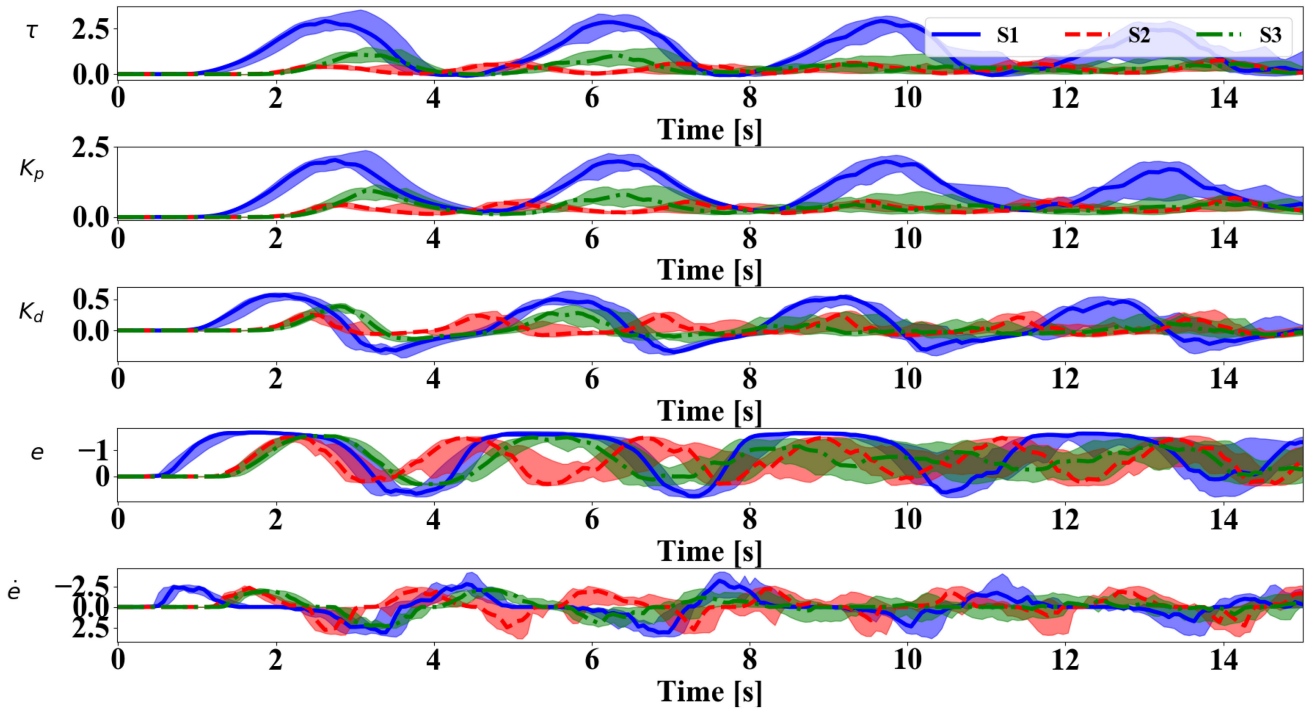

Fig. 6. Statistical results of the proposed online impedance adaptation control for RAN tasks. In the tasks, three subjects (i.e., S1–S3) wore the POW-EXO, and 16 trials were run for each subject. Rows 1–5 illustrate the medians and deviations of the joint control torque τ [see (10)], impedance parameters K_p and K_d, and the position e and velocity $\dot{e}$ errors [see (5)]. Blue, red, and green colors depict the results of subjects S1–S3, respectively.

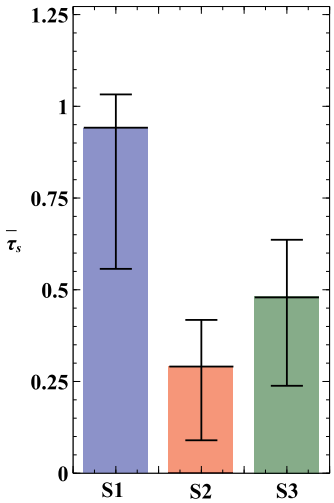

Fig. 7. Exercise involvement [see (14)] of subjects S1–S3.

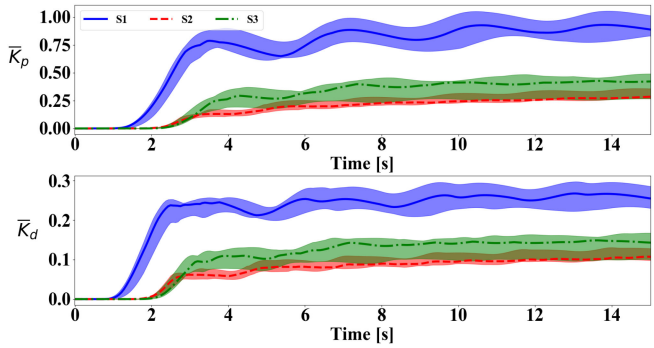

Fig. 8. Average mechanical impedance of interactive elbow control. Rows 1 and 2 show the average impedance $\overline{K}_p$ and $\overline{K}_d$ [see (15)] of the RAN controller with respect to subjects S1–S3.

where $\overline{K_p}(t)$ and $\overline{K_d}(t)$ are the moving averages of mechanical impedance parameters $K_p(t)$ and $K_d(t)$ [24], respectively. Δt is the time step, while n is the step length. The same controller has been used to quantify the finger muscle fatigue [29].

The presented OIAM can free humans from manually tuning mechanical impedance of exoskeletons for various subjects. Moreover, the control outperforms large impedance controllers in terms of its friendly interaction control and actuator dysfunction prevention. The comparison can be seen in [20].

C. Control Comparison

The proposed LBCM outperforms conventional trial–error and iterative impedance learning (i.e., TEL and ILPC) in the AAN task (see Section III-A). The comparison was performed on subject S1. We can see that the LBCM enables the POW-EXO to achieve fewer position errors [see $\overline{e}$ in Fig. 10(a) and (b)], compared to the ILPC and TEL. This is because its impedance adaptation mechanism online modulates interaction impedance terms based on position and velocity errors. Such a modulation makes the LBCM start at a smaller position error, compared to the ILPC and TEL. Note that the TEL and ILPC were revised based on their origins, such that the

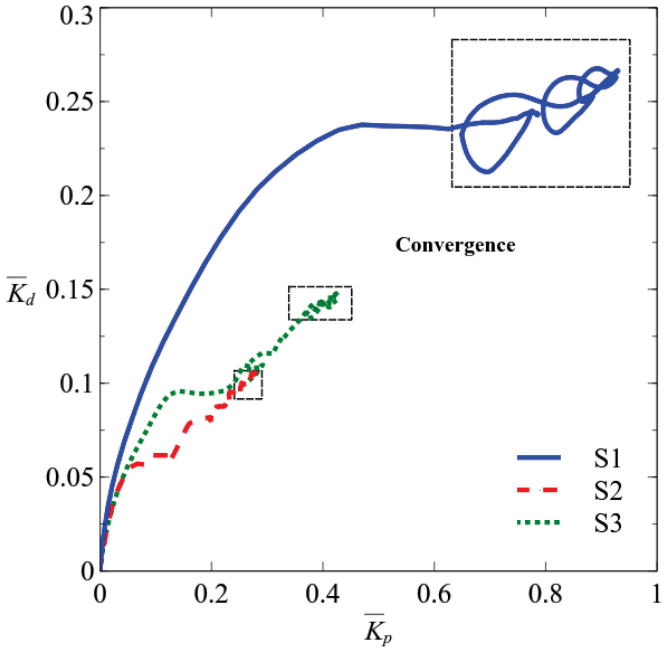

Fig. 9. Variance and invariance (convergence, see the black dashed rectangles) of average mechanical impedance of interactive elbow control with respect to subjects S1–S3. The blue, red, and green lines denote the medians of the average impedance $\overline{K}_p$ and $\overline{K}_d$ (see Fig. 8).

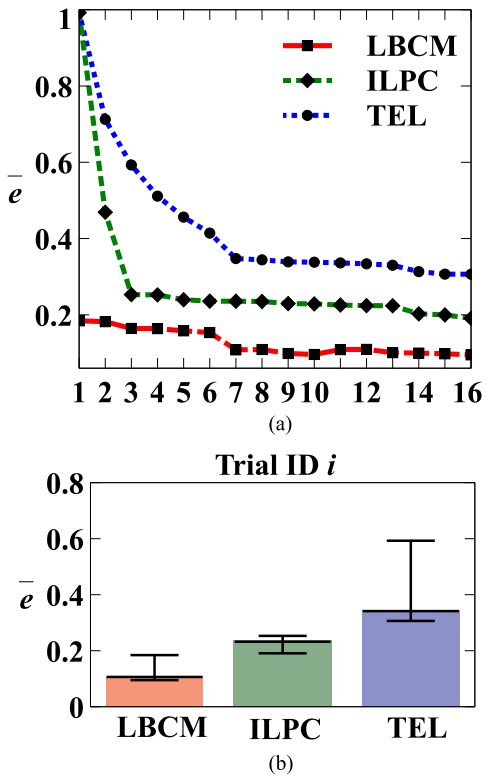

Fig. 10. Control comparison between our and SOA controllers. It was performed on subject S1.

TABLE II
COMPARISON BETWEEN OUR PROPOSED AND SOA METHODS

Method		Ours	Lotti [19]	Zhijun [33]	Li [9]	Proietti [13]
Function	AAN	Yes	Yes	Yes	Yes	Yes
	RAN	Yes	No	No	No	No
	IIQ	Yes	No	No	No	No
Control	Torque	Yes	No	No	Yes	Yes
	Angle/velocity	No	Yes	Yes	No	No
	Predictive feed-forward learning	Yes	No	No	Yes	Yes
	Online stiffness and damping adaptation	Yes	No	No	No	No
Required sensing	EMG	No	Yes	No	No	No
	Force/torque	No	Yes	Yes	No	No
	Joint position	Yes	Yes	Yes	Yes	Yes
	Joint velocity	Yes	Yes	Yes	Yes	Yes

predictive (i.e., τ_{ff}) and adaptive (i.e., K_p and K_d) terms are learned for a suitable comparison (see their implementations in Section IV).

IV. CONCLUSION

The majority of this article focuses on our novel learning-based model achieved for multifunctional elbow exoskeleton control. However, it is helpful to discuss and conclude its contribution to SOA methods and future extensions. First, most SOA methods rely heavily on additional external sensing, such as EMG and force [14], [15]. However, these sensors are subject to the following intrinsic limitations.

1) Their signals are inherently noisy and vary in accordance with different applications [12].
2) An activated muscle contributes to various limb movements, leading to the inaccurate prediction of wearers' intentions [30].
3) The external sensing becomes less precise when wearers perspire and sensors fall out [5].
4) Estimating the interaction torques from the EMG and force signals of patients can be difficult owing to an abnormal EMG–torque relationship [31], [32].

These limitations may reduce learning and control robustness of SAO position/velocity [19], [33] and torque [9], [17] methods for different tasks and wearers. To address these limitations, predictive learning and online (impedance) adaptation control were integrated to exclude EMG and force sensors in our proposed model. Its implementation relied only on the joint position and velocity feedback, thereby enhancing exoskeleton learning-based control robustness (see detailed comparisons in Table II). Our impedance control is better suited for friendly exoskeleton and human interaction control [10], [11], compared to position/velocity (admittance) control [19], [33]. Second, our proposed model allows an elbow exoskeleton to provide two functions to patients in different rehabilitation stages. This greatly increases exoskeletons' affordability and productivity in home-based applications, compared to the conventional single-function one.

Our core scientific contribution is online stiffness and damping adaptation mechanism, providing a novel way to achieve multifunctional exoskeleton control, as well as interactive (mechanical) impedance quantification (IIQ, see Table II). The mechanism enables our proposed method to have lower sensory dependence than classical angle/velocity (admittance) control [19], [33], and handle nonrepeatable arm movement dynamics better than conventional variable impedance controllers [9], [13] (see Fig. 10). Their stiffness K_p and damping K_d gains are modulated based on previous (trial) tracking errors [see (16) and (17)]. "Nonrepeatable" here means a subject would not repeat the same involuntary arm feedback in task trials, leading to unknown and different arm dynamics.

Despite the presented effectiveness, the proposed model still requires improvement. First, the model can be extended for multijoint exoskeleton control. A possible solution is to extend the model for Cartesian control of multijoint exoskeletons. Second, the model can be revised for applications to hybrid exoskeletons consisting of passive and active actuation. The terms (e.g., impedance K_p and K_d) for active actuation will be online learned to work with passive (e.g., physical springs) in terms of energy-efficient exoskeleton control.

Appendix
Compared Learning-Based Control

A. Trial-and-Error Learning (TEL)

Comparable to human sensorimotor learning control, motor errors are used to tune motor commands in the TEL. The trial error is used to increase exoskeleton assistance, if a subject does not achieve task minimization. Based on the error $\overline{e}^{i-1}$, parameters $\theta = [\tau_{\text{ff}}, K_p, K_d]^T$ at the ith trial are learned by

$$\begin{aligned} &\tau_{\text{ff}}^i = \tau_{\text{ff}}^{i-1} + \lambda \overline{e}^{i-1}, K_p^i = K_p^{i-1} + \lambda \overline{e}^{i-1}, \lambda = 0.2 \\ &K_d^i = \mu k_p^i, \mu = 0.2 \end{aligned} \tag{16}$$

where the learning rate λ and ratio μ were empirically chosen to achieve fast stable learning-based exoskeleton control. The learning law is revised from the one presented in [13], in which there is no feedforward term (i.e., τ_{ff}). Although the original law was proposed to maximize subjects' involvement, it is still a classical TEL impedance control model for adaptive control aimed by the presented AAN control task.

B. Iterative Learning Impedance Control (ILPC)

In contrast to TEL learning [see (16)], parameters $\theta = [\tau_{\text{ff}}, K_p, K_d]^T$ in the ILPC are tuned over the time steps of a trial. The ILPC mimics human sensorimotor learning in physical interaction control [24]. Humans tend to modulate their feedforward motor and feedback impedance control commands in unstable interactive tasks (e.g., tooling) [23]. The modulation is based on the simultaneous minimization of feedforward and feedback effort, leading to an iterative learning impedance control law

$$\begin{aligned} \tau_{\text{ff}}^i(t) &= \tau_{\text{ff}}^{i-1}(t) + Q_F[\varepsilon(t) - \beta(t)\tau_{\text{ff}}^{i-1}(t)] \\ K_p^i(t) &= K_p^{i-1}(t) + Q_P[\varepsilon(t)e(t) - \beta(t)K_p^{i-1}(t)] \\ K_d^i &= K_d^{i-1}(t) + Q_D[\varepsilon(t)\dot{e}(t) - \beta(t)K_d^{i-1}(t)] \end{aligned} \tag{17}$$

where learning rates are set as follows: $Q_F = 0.5$, $Q_P = 0.2$, and $Q_D = 0.2$. The rates were empirically chosen to achieve fast stable elbow exoskeleton control. The stability proof of the learning law [i.e., (17)] refers to [34]. A similar learning law has been applied to robotic rehabilitation [9]. The position $e(t)$ and velocity $\dot{e}(t)$ errors can be seen in (5), while factor $\beta(t)$ is given in (7).

Acknowledgment

The authors would like to thank the volunteers for participating in the experiments.

References

[1] K. Inagaki, "Current concepts of elbow-joint disorders and their treatment," *J. Orthopaedic Sci.*, vol. 18, no. 1, pp. 1–7, 2013.
[2] T. S. Ellenbecker, B. Pluim, S. Vivier, and C. Sniteman, "Common injuries in tennis players: Exercises to address muscular imbalances and reduce injury risk," *Strength Conditioning J.*, vol. 31, no. 4, pp. 50–58, 2009.
[3] B. R. Brewer, S. K. McDowell, and L. C. Worthen-Chaudhari, "Poststroke upper extremity rehabilitation: A review of robotic systems and clinical results," *Topics Stroke Rehabil.*, vol. 14, no. 6, pp. 22–44, Dec. 2007.
[4] K. Lo, M. Stephenson, and C. Lockwood, "The economic cost of robotic rehabilitation for adult stroke patients: A systematic review," *JBI Evidence Synth.*, vol. 17, no. 4, pp. 520–547, 2019.
[5] M. A. Gull, S. Bai, and T. Bak, "A review on design of upper limb exoskeletons," *Robotics*, vol. 9, no. 1, pp. 1–35, 2020.
[6] A. U. Pehlivan, D. P. Losey, and M. K. O'Malley, "Minimal assist-as-needed controller for upper limb robotic rehabilitation," *IEEE Trans. Robot.*, vol. 32, no. 1, pp. 113–124, Feb. 2016.
[7] S. Zhang *et al.*, "Integrating compliant actuator and torque limiter mechanism for safe home-based upper-limb rehabilitation device design," *J. Med. Biol. Eng.*, vol. 37, no. 3, pp. 357–364, 2017.
[8] M. Hamaya, T. Matsubara, T. Noda, T. Teramae, and J. Morimoto, "Learning assistive strategies for exoskeleton robots from user-robot physical interaction," *Pattern Recognit. Lett.*, vol. 99, pp. 67–76, 2017.
[9] Y. Li, X. Zhou, J. Zhong, and X. Li, "Robotic impedance learning for robot-assisted physical training," *Front. Robot. AI*, vol. 6, p. 78, 2019, doi: 10.3389/frobt.2019.00078.
[10] T. Proietti, V. Crocher, A. Roby-Brami, and N. Jarrassé, "Upper-limb robotic exoskeletons for neurorehabilitation: A review on control strategies," *IEEE Rev. Biomed. Eng.*, vol. 9, pp. 4–14, 2016, doi: 10.1109/RBME.2016.2552201.
[11] C. Ott, R. Mukherjee, and Y. Nakamura, "A hybrid system framework for unified impedance and admittance control," *J. Intell. Robot. Syst.*, vol. 78, no. 3, pp. 359–375, 2015.
[12] A. M. Khan, D. Yun, M. A. Ali, J. Han, K. Shin, and C. Han, "Adaptive impedance control for upper limb assist exoskeleton," in *Proc. IEEE Int. Conf. Robot. Automat.*, 2015, pp. 4359–4366.
[13] T. Proietti, G. Morel, A. Roby-Brami, and N. Jarrassé, "Comparison of different error signals driving the adaptation in assist-as-needed controllers for neurorehabilitation with an upper-limb robotic exoskeleton," in *Proc. IEEE Int. Conf. Robot. Automat.*, 2017, pp. 6645–6650.
[14] M. R. U. Islam and S. Bai, "Payload estimation using forcemyography sensors for control of upper-body exoskeleton in load carrying assistance," *Model., Identification Control*, vol. 40, no. 4, pp. 189–198, 2019.
[15] Z. Li, Z. Huang, W. He, and C. Su, "Adaptive impedance control for an upper limb robotic exoskeleton using biological signals," *IEEE Trans. Ind. Electron.*, vol. 64, no. 2, pp. 1664–1674, Feb. 2017.
[16] R. Meattini, D. Chiaravalli, G. Palli, and C. Melchiorri, "sEMG-based human-in-the-loop control of elbow assistive robots for physical tasks

and muscle strength training," *IEEE Robot. Automat. Lett.*, vol. 5, no. 4, pp. 5795–5802, Oct. 2020.
[17] T. Teramae, T. Noda, and J. Morimoto, "EMG-based model predictive control for physical human-robot interaction: Application for assist-as-needed control," *IEEE Robot. Automat. Lett.*, vol. 3, no. 1, pp. 210–217, Jan. 2018.
[18] S. K. Manna and V. N. Dubey, "Comparative study of actuation systems for portable upper limb exoskeletons," *Med. Eng. Phys.*, vol. 60, pp. 1–13, 2018.
[19] N. Lotti *et al.*, "Adaptive model-based myoelectric control for a soft wearable arm exosuit: A new generation of wearable robot control," *IEEE Robot. Automat. Mag.*, vol. 27, no. 1, pp. 43–53, Mar. 2020.
[20] X. Xiong and P. Manoonpong, "Online adaptive resistance control of an arm exercise exoskeleton," in *Proc. Robots Hum. Life- Proc. 23rd Int. Conf. Climbing Walking Robots Support Technol. Mobile Mach.*, 2020, pp. 31–38.
[21] X. Zhang, S. Wang, J. B. Hoagg, and T. M. Seigler, "The roles of feedback and feedforward as humans learn to control unknown dynamic systems," *IEEE Trans. Cybern.*, vol. 48, no. 2, pp. 543–555, Feb. 2018.
[22] R. S. Maeda, T. Cluff, P. L. Gribble, and J. A. Pruszynski, "Feedforward and feedback control share an internal model of the arm's dynamics," *J. Neurosci.*, vol. 38, no. 49, pp. 10505–10514, Dec. 2018.
[23] D. W. Franklin, "Impedance control: Learning stability in human sensorimotor control," in *Proc. 37th Annu. Int. Conf. IEEE Eng. Med. Biol. Soc.*, 2015, pp. 1421–1424.
[24] J. Mizrahi, "Mechanical impedance and its relations to motor control, limb dynamics, and motion biomechanics," *J. Med. Biol. Eng.*, vol. 35, no. 1, pp. 1–20, 2015.
[25] X. Xiong and P. Manoonpong, "Adaptive motor control for human-like spatial-temporal adaptation," in *Proc. IEEE Int. Conf. Robot. Biomimetics*, 2018, pp. 2107–2112.
[26] X. Xiong and P. Manoonpong, "Resistance-as-needed (RAN) control for a wearable and soft hand exoskeleton," *Gait Posture*, vol. 81, pp. 398–399, 2020.
[27] X. Xiong, "Multifunctional elbow exoskeleton control," Accessed: Jan. 7, 2021. [Online]. Available: https://www.youtube.com/watch?v=oFDWYAt9tz8
[28] B. Hwang, B. M. Oh, and D. Jeon, "An optimal method of training the specific lower limb muscle group using an exoskeletal robot," *IEEE Trans. Neural Syst. Rehabil. Eng.*, vol. 26, no. 4, pp. 830–838, Apr. 2018.
[29] X. Xiong and P. Manoonpong, "A variable soft finger exoskeleton for quantifying fatigue-induced mechanical impedance," in *Proc. IEEE Int. Conf. Robot. Automat.*, 2021.
[30] K. Kiguchi and Y. Hayashi, "An EMG-based control for an upper-limb power-assist exoskeleton robot," *IEEE Trans. Syst., Man, Cybern., Part B (Cybern.)*, vol. 42, no. 4, pp. 1064–1071, Aug. 2012.
[31] M. Bhadane, J. Liu, W. Z. Rymer, P. Zhou, and S. Li, "Re-evaluation of EMG-torque relation in chronic stroke using linear electrode array EMG recordings," *Sci. Rep.*, vol. 6, no. 1, 2016, Art. no. 28957, doi: 10.1038/srep28957.
[32] O. J. Tate and D. L. Damiano, "Torque-EMG relationships in normal and spastic muscles," *Electromyogr. Clin. Neuriophysiol.*, vol. 42, no. 6, pp. 347–357, Sep. 2002.
[33] Z. Li, B. Huang, Z. Ye, M. Deng, and C. Yang, "Physical human-robot interaction of a robotic exoskeleton by admittance control," *IEEE Trans. Ind. Electron.*, vol. 65, no. 12, pp. 9614–9624, Dec. 2018.
[34] Y. Li, G. Ganesh, N. Jarrassé, S. Haddadin, A. Albu-Schaeffer, and E. Burdet, "Force, impedance, and trajectory learning for contact tooling and haptic identification," *IEEE Trans. Robot.*, vol. 34, no. 5, pp. 1170–1182, Oct. 2018.

Xiaofeng Xiong was born in Hainan, China. He received the Ph.D. degree in computer science from Georg-August-Universität Göttingen, Göttingen, Germany, in 2015.

After working in Göttingen Medical Center and Hamburg University, he is currently an Assistant Professor with the SDU Biorobotics, Odense, Denmark. His current research interests include learning-based robot control, motor control and learning, and neuromechanical modeling.

Dr. Xiong was the recipient of the Emerald Innovation and CLAWAR Best Technical Paper Awards.

Cao Danh Do received the M.Sc. degree in structural engineering from University of Southern Denmark (SDU), Odense, Denmark, in 2014.

He is currently a Research Assistant with the SDU Biorobotics, Odense, Denmark. During the last two years, his focus has shifted toward contributing to designing and building bio-inspired robots and other mechanisms through the prototyping activities. His current research interests include mechanism design, fabrication methods, rapid prototyping, and topology optimization.

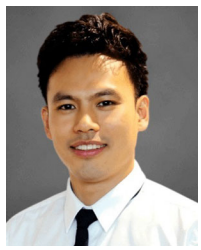

Poramate Manoonpong (Member, IEEE) received the Ph.D. degree in electrical engineering and computer science from the University of Siegen, Siegen, Germany, in 2006.

He is currently a Professor of Biorobotics with the University of Southern Denmark (SDU), Denmark, and a Professor with the School of Information Science and Technology, Vidyasirimedhi Institute of Science and Technology, Rayong, Thailand. His current research interests include embodied AI, machine learning for robotics, and neural locomotion control of walking machines.